Biogeosciences Discuss., https://doi.org/10.5194/bg-2018-258
Manuscript under review for journal Biogeosciences
Discussion started: 12 July 2018

Biogeosciences Discussions Open Access EGU

Export flux of unprocessed atmospheric nitrate from temperate forested catchments: A possible new index for nitrogen saturation

Fumiko Nakagawa[1], Urumu Tsunogai[1], Yusuke Obata[1], Kenta Ando[1], Naoyuki Yamashita[2$], Tatsuyoshi Saito[2&], Shigeki Uchiyama[2#], Masayuki Morohashi[2], Hiroyuki Sase[2]

[1]Graduate School of Environmental Studies, Nagoya University, Furo-cho, Chikusa-ku, Nagoya 464-8601, Japan.
[2]Asia Center for Air Pollution Research, 1182 Sowa, Nishi-ku, Niigata-shi, Niigata 950-2144, Japan.
[$]Present address: Forestry and Forest Products Research Institute, Tsukuba, Ibaraki 305-8687, Japan.
[&]Present address: Niigata Prefectural Institute of Public Health and Environmental Sciences, 314-1 Sowa, Nishi-ku, Niigata-Shi, Niigata 950-2144, Japan.
[#]Present address: Ministry of Agriculture, Forestry and Fisheries, 1-2-1, Kasumigaseki, Chiyoda-ku, Tokyo 100-8950, Japan.

Correspondence to: Urumu Tsunogai (urumu@nagoya-u.jp)

Abstract. To clarify the biological processing of nitrate within temperate forested catchments using unprocessed atmospheric nitrate exported from each catchment as a tracer, we continuously monitored stream nitrate concentrations and stable isotopic compositions including ^{17}O-excess (Δ^{17}O) in three forested catchments in Japan (KJ, IJ1, and IJ2) for more than two years. The catchments showed varying flux-weighted average nitrate concentrations: 58.4, 24.4, and 17.1 μmol L^{-1} in KJ, IJ1, and IJ2, respectively. In addition to stream nitrate, nitrate concentrations and stable isotopic compositions in soil water were determined for comparison in the most nitrate-enriched catchment (the KJ site). While ^{17}O-excess of nitrate in soil water showed significant seasonal variation, ranging from +0.1 to +5.7‰, stream nitrate showed small variation, from +0.8 to +2.0‰ in KJ, +0.7 to +2.8‰ in IJ1, and +0.4 to +2.2‰ in IJ2. We concluded that the major source of stream nitrate in each forested catchment was nitrate in groundwater, which buffered the seasonal variations in soil water nitrate. The estimated annual export flux of unprocessed atmospheric nitrate

Biogeosciences Discuss., https://doi.org/10.5194/bg-2018-258
Manuscript under review for journal Biogeosciences
Discussion started: 12 July 2018

accounted for 9.4±2.6%, 6.5±1.8%, and 2.6±0.6% of the annual deposition flux of atmospheric nitrate in KJ, IJ1, and IJ2, respectively. The export flux of unprocessed atmospheric nitrate relative to the deposition flux showed a clear normal correlation with the flux-weighted average concentration of stream nitrate, indicating that reductions in the biological assimilation rates of nitrate in forested soils, rather than increased nitrification rates, are likely responsible for the enrichment of stream nitrate, probably due to nitrogen saturation. The export flux of unprocessed atmospheric nitrate relative to the deposition flux in each forest ecosystem is applicable as an index for nitrogen saturation.

1 Introduction

1.1 Stream nitrate being exported from forested watersheds

Nitrate is the representative nitrogen nutrient for primary production in aquatic environments. As a result, an excess of nitrate in stream water can cause significant ecological and economic problems, such as eutrophication in downstream areas including receiving lakes, estuaries, and oceans (McIsaac et al., 2001; Paerl, 2009).

Forested ecosystems have traditionally been considered nitrogen-limited. However, probably due to elevated nitrogen loading through atmospheric deposition, some forested ecosystems become nitrogen-saturated (Aber et al., 1989), from which elevated levels of nitrate are exported (Peterjohn et al., 1996; Wright and Tietema, 1995). Either increased nitrification rates in forested soils or reductions in N retention are assumed to be responsible for both enhanced nitrogen leaching from soils and the increased export flux of nitrate in nitrogen-saturated watersheds (Peterjohn et al., 1996).

Nitrate concentrations in stream water are controlled through the complicated interplay between several processes within a catchment including: (1) the addition of atmospheric nitrate ($NO_3^-{}_{atm}$) through deposition, (2) the production of nitrate through microbial nitrification in soils, (3) the removal of nitrate through assimilation by plants and microbes, and (4) the removal of nitrate

through denitrification by microbes. Therefore, interpretation of the processes regulating nitrate concentrations in stream water is not always straightforward, including the elevated nitrate concentrations in the streams eluted from nitrogen-saturated forested catchments.

The natural stable isotopic compositions of nitrate ($\delta^{15}N$ and $\delta^{18}O$) have been widely used to determine the origin and behavior of nitrate in stream water (Durka et al., 1994; Kendall, 1998). In addition to these traditional isotopes, ^{17}O-excess ($\Delta^{17}O$; the definition will be presented in section 1.2) of nitrate has been used as an additional, more robust tracer for unprocessed $NO_3^-{}_{atm}$ (nitrate that had been supplied via atmospheric deposition and have survived the biological processing of nitrate, such as assimilation and denitrification, within surface ecosystems) in stream water in recent years (Bourgeois et al., 2018; Michalski et al., 2004; Riha et al., 2014; Sabo et al., 2016; Tsunogai et al., 2010; Tsunogai et al., 2014; Tsunogai et al., 2016). By determining both concentration and the ^{17}O-excess of stream nitrate, we can quantify unprocessed $NO_3^-{}_{atm}$ in stream water accurately and precisely. Recent studies on nitrate including unprocessed $NO_3^-{}_{atm}$ exported from forested catchments via streams during base flow period have revealed that the export flux of unprocessed $NO_3^-{}_{atm}$ increases in accordance with increases in the stream nitrate concentration (Rose et al., 2015a; Rose et al., 2015b; Tsunogai et al., 2014). These results implied that unprocessed $NO_3^-{}_{atm}$ exported from forested catchments can be used as a tracer to identify the biological processing of nitrate in each catchment area and to clarify the processes regulating nitrate concentrations in stream water.

In this study, we monitored both concentrations and stable isotopic compositions (including $\Delta^{17}O$) of stream nitrate exported from three forested catchments in Japan for more than 2 years. The studied catchments were chosen so that the average nitrate concentrations in the streams varied. In addition to nitrate in streams, the nitrate concentrations and stable isotopic compositions in soil water were determined over the same observation period for comparison in one catchment. Based on the differences in the export flux of unprocessed $NO_3^-{}_{atm}$ between the catchments, we aimed to clarify the processes regulating nitrate concentrations in stream water exported from temperate forested watersheds, with special emphasis on the relationship with nitrogen saturation.

Biogeosciences Discuss., https://doi.org/10.5194/bg-2018-258
Manuscript under review for journal Biogeosciences
Discussion started: 12 July 2018

1.2 ^{17}O-excess of nitrate

The natural stable isotopic compositions of nitrate are $\delta^{15}N$, $\delta^{17}O$, and $\delta^{18}O$. The delta (δ) values are calculated by $R_{sample}/R_{standard} - 1$, where R is the $^{18}O/^{16}O$ ratio for $\delta^{18}O$ (or the $^{17}O/^{16}O$ ratio for $\delta^{17}O$ or the $^{15}N/^{14}N$ ratio for $\delta^{15}N$) in both the sample and the respective international standard (air N_2 for nitrogen and Vienna standard mean ocean water (VSMOW) for oxygen). Atmospheric nitrate, which is produced via photochemical reactions between atmospheric NO and O_3, can be characterized by the anomalous enrichment in ^{17}O compared to remineralized nitrate ($NO_3^-{}_{re}$), which is produced from organic nitrogen through general chemical reactions including microbial N mineralization and microbial nitrification in the biosphere (Alexander et al., 2009; Michalski et al., 2003; Morin et al., 2008; Tsunogai et al., 2010; Tsunogai et al., 2016). By using the $\Delta^{17}O$ signature (the magnitude of ^{17}O-excess) defined by the following equation (Kaiser et al., 2007; Miller, 2002), we can distinguish unprocessed $NO_3^-{}_{atm}$ ($\Delta^{17}O > 0$) from $NO_3^-{}_{re}$ ($\Delta^{17}O$ close to 0):

$$\Delta^{17}O = \frac{1+\delta^{17}O}{\left(1+\delta^{18}O\right)^{\beta}} - 1,$$

where the constant β is 0.5279 (Kaiser et al., 2007; Miller, 2002).

Continuous monitoring of the $\Delta^{17}O$ value of $NO_3^-{}_{atm}$ deposited at mid-latitudes has clarified that the annual average $\Delta^{17}O$ value of $NO_3^-{}_{atm}$ is almost constant (Alexander et al., 2009; Kaiser et al., 2007; Michalski et al., 2003; Nelson et al., 2018; Tsunogai et al., 2010; Tsunogai et al., 2016). In addition, $\Delta^{17}O$ is stable during the mass-dependent isotope fractionation processes within surface ecosystems (Miller, 2002; Thiemens et al., 2001). Therefore, while the $\delta^{15}N$ or $\delta^{18}O$ signature of $NO_3^-{}_{atm}$ can be overprinted by biological processes subsequent to deposition, $\Delta^{17}O$ can be used as a robust tracer of unprocessed $NO_3^-{}_{atm}$ to reflect its accurate mole fraction within total NO_3^- regardless of partial metabolism through denitrification and assimilation subsequent to deposition (Michalski et al., 2004; Tsunogai et al., 2011; Tsunogai et al., 2014), using the following equation:

$$\frac{C_{atm}}{C_{total}} = \frac{\Delta^{17}O}{\Delta^{17}O_{atm}},$$

where C_{atm} and C_{total} denote the concentrations of unprocessed $NO_3^-{}_{atm}$ and NO_3^- in each water sample, and $\Delta^{17}O_{atm}$ and $\Delta^{17}O$ denote the $\Delta^{17}O$ values of $NO_3^-{}_{atm}$ and total nitrate in each water sample, respectively. This is the primary advantage of using the $^{17}O/^{16}O$ ratio as an additional tracer of unprocessed $NO_3^-{}_{atm}$. In this study, we used the average $\Delta^{17}O$ value of $NO_3^-{}_{atm}$ obtained at the nearby Sado-seki monitoring station during the observation period from April 2009 to March 2012 ($\Delta^{17}O_{atm}$ = +26.3‰; Tsunogai et al., 2016) for $\Delta^{17}O_{atm}$ in Eq. (2) to estimate C_{atm} in the study streams allowing an error range of 3‰ (Tsunogai et al., 2016).

Moreover, additional measurements of the $\Delta^{17}O$ values of nitrate together with $\delta^{18}O$ enable us to exclude the contribution of unprocessed $NO_3^-{}_{atm}$ in the determined $\delta^{18}O$ values and to estimate the corrected $\delta^{18}O$ values ($\delta^{18}O_{re}$) for accurate evaluation of the source and behaviour of $NO_3^-{}_{re}$, including anthropogenically produced $NO_3^-{}_{re}$ (Dejwakh et al., 2012; Liu et al., 2013; Riha et al., 2014; Tsunogai et al., 2011; Tsunogai et al., 2010; Tsunogai et al., 2014; Tsunogai et al., 2016).

2 Experimental Section

2.1 Site description

In this study, we determined the export flux of unprocessed $NO_3^-{}_{atm}$ through continuous monitoring of stream water in three forested catchments in Japan: a catchment (KJ site) in the Kajikawa forested watershed and two subcatchments (IJ1 and IJ2 sites) in the Lake Ijira watershed (Fig. 1(a)). The deposition rate of $NO_3^-{}_{atm}$ was determined for each catchment by collecting samples of deposition outside the forest canopy. Soil water samples were also collected from the KJ site.

The KJ site is located in the northern part of Shibata city, Niigata Prefecture, near the coast of the Japan Sea (Fig. 1(a)). The forest is composed of Japanese cedars (*Cryptomeria japonica*) approximately 40 years old in 2012 (Sase et al., 2012). This site is characterized by perhumid climate conditions with no clear dry season during the year. The daily air temperature in the region varies from –2 °C to +34 °C, with an annual mean of 13 °C during the observation period of this study. The annual mean precipitation was around 2500 mm. The site usually experiences snowfall from late December to March with the maximum depth exceeding 100 cm, even on the slope. The

Biogeosciences Discuss., https://doi.org/10.5194/bg-2018-258
Manuscript under review for journal Biogeosciences
Discussion started: 12 July 2018

studied catchment is 3.84 ha with an elevation from 60 to 170 m above sea level (Fig. 1(b)). The catchment is characterized by a high loading rate of atmospheric nitrogen, as well as nitrate enrichment of more than 50 μmol L^{-1} in the stream water eluted from the catchment. Kamisako et al. (2008) proposed that atmospheric nitrogen inputs are exceeding the biological demand at this site. As a result, we chose this catchment to study unprocessed $NO_3^-{}_{atm}$ as a tracer as it is an example of a catchment enriched in stream nitrate. Details of the Kajikawa experimental forest have been described in past studies (Kamisako et al., 2008; Sase et al., 2012; Sase et al., 2008).

Lake Ijira (Fig. 2) is a reservoir constructed on one of the tributaries of the Nagara river in the Gifu prefecture, Honshu, Japan. The mean annual precipitation is around 3300 mm. The precipitation regime is characterized by relatively wet springs and summers (200 mm $month^{-1}$ from April to September) and relatively dry winters (about 100 mm $month^{-1}$ from December to February). The daily air temperature in the region varies from –3 °C to +31 °C, with an annual mean of 13 °C. The site is covered with snow from December to March every year.

The Kamagadani catchment (IJ1 site; 298 ha) and the Kobora catchment (IJ2 site; 108 ha) in the Lake Ijira watershed were studied as well (Fig. 2). The dominant vegetation in the Kamagadani catchment (IJ1) is Japanese cypress (*Chamaecyparis obtusa*, 49 %), followed by broadleaf trees (29 %), Japanese red pine (*Pinus densiflora*, 13 %), and Japanese cedar (*Cryptomeria japonic*a, 8%), while the dominant vegetation in the Kobora catchment (IJ2) is Japanese red pine (*Pinus densiflora*, 46 %), followed by broadleaf trees (30 %), Japanese cypress (*Chamaecyparis obtusa*, 17 %), and Japanese cedar (*Cryptomeria japonic*a, 7 %). Japanese cypress and Japanese cedar stands are plantation forests, which were aged mainly from 15 to 25 years and 30 to 45 years, respectively, in 1998. The red pine and broadleaf stands are secondary forests. Major tree species in secondary broadleaf forests are *Clethra barbinervis*, *Quercus serrata*, *Ilex pedunculosa*, *Quercus variabilis*, *Carpinus tschonoskii*, *Acer mono*, and *Quercus glauca*.

The annual wet deposition flux of $NO_3^-{}_{atm}$ in the Lake Ijira watershed was the highest of all EANET deposition monitoring sites in Japan (Yamada et al., 2007), probably because the catchment is located only about 40 km north of Nagoya and the surrounding industrial area (Chukyo industrial

area). As a result, the discharge rate, water temperature, pH, electrical conductivity (EC), and alkalinity have been measured continuously at the outlets of the IJ1 and IJ2 (RW1 and RW3, respectively, in Fig. 2) since 1988 (Nakahara et al., 2010). For this reason, we chose the Lake Ijira watershed for this study. Details of the Lake Ijira watershed have been described in past studies (Nakahara et al., 2010; Yamada et al., 2007).

2.2 Stream water and discharge rates

Samples of stream water were collected at the weir located at the outlet of each catchment (KJ, IJ1, and IJ2) about once a month between May 2012 and December 2014 in KJ and from March 2012 to December 2014 in IJ1 and IJ2.

At the KJ site, a V-notch weir (half angle: 30°) and a partial flume were installed at the bottom of the catchment (Fig. 1(b)) where the stream water was collected. The data from the V-notch weir was used to measure the discharge rate. At the IJ1 site, the discharge rates were calculated from both water depth and flow velocity at each weir. The water depth was measured at 100 cm intervals across the river flow, and the flow velocity was measured at the midpoints of each 100 cm split using a flow meter (CM-10S, Toho Dentan, Tokyo, Japan). At the IJ2 site, the discharge rates were estimated from the calculated values from IJ1, assuming that the discharge rates from both sites varied in proportion to the area of the catchments.

2.3 Soil water

Soil water samples were collected at two stations (SLS and SMS; Fig. 1(b)) within the KJ catchment on average once every six weeks from December 2012 to December 2014, using porous cup soil solution samplers (DIK-8390-11/DIK-8390-58, DAIKI, Japan). Because the site is covered with snow in winter, however, a limited number of samples were taken between December to March.

The SLS station is located by the stream side, while the SMS station is located about 20 m away from the SLS station to the northeast direction (Fig. 1(b)). The SMS is 23m higher than SLS in

altitude. The soil water samples were collected at a depth of 20 cm at each station (SLS 20 and SMS 20). Soil water samples were also collected at a depth of 60 cm at the SLS station (SLS 60).

2.4 Atmospheric nitrate deposition rates

For the KJ site, a filtering-type bulk deposition sampler with a funnel (200 mm diameter) installed in an open field outside the forest canopy on the northern ridge of the catchment (Fig. 1(b)) was used to determine the areal deposition flux of $NO_3^-{}_{atm}$ (Kamisako et al., 2008; Sase et al., 2008). Using the sampler, bulk depositions were collected into sample bottles at intervals of about four weeks. Sample bottles were covered with aluminum foil or enclosed in a polystyrene foam box to avoid light and suppress algal growth during storage in the field. The volume of each sample was determined using plastic cylinders in the field, and portions of each sample were brought to the laboratory for further analysis. Please note that the dry deposition flux, especially for gaseous HNO_3, is underestimated in the $NO_3^-{}_{atm}$ deposition flux determined through this method (Aikawa et al., 2003), while the deposition flux of $NO_3^-{}_{atm}$ could be overestimated due to the progress of nitrification in sample bottles during storage in the field until recovery (Clow et al., 2015).

For the IJ1 and IJ2 sites, data on the areal $NO_3^-{}_{atm}$ deposition flux determined separately for wet and dry deposition at the outlet of IJ1 (140 m above sea level; Fig. 2) and reported by EANET (EANET, 2014, 2015), were used in this study. The dry deposition flux was calculated from the concentrations of particulate nitrate and gaseous HNO_3 in air.

2.5 Analysis

Samples of stream water (KJ, IJ1, and IJ2), soil water (KJ), and deposition (KJ) were transported to the laboratory within 1 h after collection and were passed through a membrane filter (pore size, 0.45 μm) and stored in a refrigerator (4 °C) until chemical analysis. The concentrations of NO_3^- were measured by ion chromatography (DX-500, Dionex Inc., USA), together with major anions and cations. Samples were analyzed within a few weeks of sampling then sealed in 50 or 100 mL polyethylene bottles for further analysis, including measurement of the isotopes in the stream and

soil water samples reported in this study. Prior to isotope analysis, the NO_3^- concentration of each stream water sample was determined again by ion chromatography to exclude samples that had been altered during storage. The longest storage period between bottling and isotope analysis was two years. None of the samples determined in this study showed significant NO_3^- deterioration or contamination during storage.

The $\delta^{18}O$ values of H_2O in the stream and soil water samples were analyzed using the cavity ring-down spectroscopy method by employing an L2120-i instrument (Picarro Inc., Santa Clara, CA, USA) equipped with an A0211 vaporizer and autosampler. The error (standard error of the mean) in this method was ± 0.1‰. Both the VSMOW and standard light Antarctic precipitation (SLAP) were used to calibrate the values to the international scale.

To determine the stable isotopic compositions of NO_3^- in the stream and soil water samples, NO_3^- in each sample was chemically converted to N_2O using a method originally developed to determine the $^{15}N/^{14}N$ and $^{18}O/^{16}O$ ratios of seawater and freshwater NO_3^- (McIlvin and Altabet, 2005) that was later modified (Konno et al., 2010; Tsunogai et al., 2008; Tsunogai et al., 2018; Yamazaki et al., 2011). In brief, the procedure was as follows. Approximately 10 mL of each sample solution was pipetted into a vial with a septum cap. Then, 0.5 g of spongy cadmium was added, followed by 150 μL of a 1 M $NaHCO_3$ solution. The sample was then shaken for 18–24 h at a rate of 2 cycles/s. Then, the sample solution was decanted into a different vial with a septum cap. After purging the solution using high purity helium, 0.4 mL of an azide/acetic acid buffer, that had also been purged using purity helium, was added. After 45 min, the solution was alkalinized by adding 0.2 mL of 6 M NaOH.

Then, the stable isotopic compositions ($\delta^{15}N$, $\delta^{18}O$, and $\Delta^{17}O$) of the N_2O in each vial were determined using the continuous-flow isotope ratio mass spectrometry (CF-IRMS) system at Nagoya University. The analytical procedures performed using the CF-IRMS system were the same as those detailed in previous studies (Hirota et al., 2010; Komatsu et al., 2008). The obtained values of $\delta^{15}N$, $\delta^{18}O$, and $\Delta^{17}O$ for the N_2O derived from the NO_3^- in each sample were compared with those derived from our local laboratory NO_3^- standards to calibrate the values of the sample NO_3^- to

an international scale and to correct for both isotope fractionation during the chemical conversion to N_2O and the progress of oxygen isotope exchange between the NO_3^--derived reaction intermediate and water (ca. 20%). The local laboratory NO_3^- standards had been calibrated using internationally distributed isotope reference materials (USGS-34 and USGS-35). In this study, we adopted the internal standard method (Nakagawa et al., 2013; Tsunogai et al., 2014; Tsunogai et al., 2018) for the calibration of sample NO_3^-.

To determine whether samples had deteriorated or were contaminated during storage and whether the conversion rate from NO_3^- to N_2O was sufficient, the concentration of NO_3^- in the samples was determined each time we analyzed the isotopic composition using CF-IRMS, based on the N_2O^+ or O_2^+ outputs. We adopted the $\delta^{15}N$, $\delta^{18}O$, or $\Delta^{17}O$ values only when the concentration measured via CF-IRMS correlated with the concentration measured via ion chromatography prior to isotope analysis within a difference of 10%. About 10% of all isotope analyses showed conversion efficiencies lower than this criterion. The NO_3^- in these samples was converted to N_2O again and reanalyzed for stable isotopic composition.

We repeated the analysis of $\delta^{15}N$, $\delta^{18}O$, and $\Delta^{17}O$ values for each sample at least three times to attain high precision. Most of the samples had a NO_3^- concentration of more than 10 μmol L^{-1}, which corresponded to a NO_3^- quantity greater than 100 nmol in a 10 mL sample. This amount was sufficient for determining the $\delta^{15}N$, $\delta^{18}O$, and $\Delta^{17}O$ values with high precision. For cases where the NO_3^- concentration was less than 10 μmol L^{-1}, the number of analyses was increased. Thus, all isotope values presented in this study have an error (standard error of the mean) better than ± 0.2‰ for $\delta^{15}N$, ± 0.3‰ for $\delta^{18}O$, and ± 0.1‰ for $\Delta^{17}O$.

Nitrite (NO_2^-) in the samples interferes with the final N_2O produced from NO_3^- because the chemical method also converts NO_2^- to N_2O (McIlvin and Altabet, 2005). Therefore, it is sometimes necessary to remove NO_2^- prior to converting NO_3^- to N_2O. However, in this study, all the stream and soil water samples analyzed for stable isotopic composition had NO_2^- concentrations lower than the detection limit (0.05 μmol L^{-1}). Thus, we skipped the processes for removing NO_2^-.

Biogeosciences Discuss., https://doi.org/10.5194/bg-2018-258
Manuscript under review for journal Biogeosciences
Discussion started: 12 July 2018

2.6 Possible variations in $\Delta^{17}O$ during partial removal and mixing

Because we used the power law shown in Eq. (1) for the definition of $\Delta^{17}O$, the $\Delta^{17}O$ values differ from those based on the linear definition (Michalski et al., 2002). The differences in the $\Delta^{17}O$ values would be less than 0.1‰ higher for the stream and soil water NO_3^- if we had used the linear definition for calculation.

Compared with $\Delta^{17}O$ values based on the linear definition, $\Delta^{17}O$ values based on the power law definition are more stable during mass-dependent isotope fractionation processes, so we considered the $\Delta^{17}O$ values of NO_3^- as stable, irrespective of any biological partial removal processes after deposition, such as assimilation or denitrification. On the other hand, $\Delta^{17}O$ values based on the power law definition are not conserved during mixing processes between fractions with different $\Delta^{17}O$ values, so the C_{atm}/C_{total} ratio estimated using Eq. (2) deviate slightly from the actual C_{atm}/C_{total} ratio in the samples. However, in this study, the extent of the deviations of the C_{atm}/C_{total} ratios of the stream NO_3^- was less than 0.2%, so we have disregarded this effect in the discussion.

2.7 Calculation of the atmospheric nitrate export flux from each catchment

To quantify the export flux of unprocessed $NO_3^-{}_{atm}$ from each catchment, the daily export flux of unprocessed $NO_3^-{}_{atm}$ per unit area of the catchment (F_{atm}) was calculated for each day on which the $\Delta^{17}O$ value of nitrate was determined, by applying equation (3) (Tsunogai et al., 2014):

$$F_{atm} = \frac{C_{atm} \times V}{S},$$

where C_{atm} denotes the concentration of unprocessed $NO_3^-{}_{atm}$, V denotes the daily average flow rate of stream water, and S denotes the total area of each catchment studied. The daily export fluxes of NO_3^- (F_{total}) and $NO_3^-{}_{re}$ (F_{re}) per unit area of catchment were also calculated from the NO_3^- concentration (C_{total}) and the daily average flow rate of the stream water (V) by applying equations (4) and (5):

$$F_{total} = \frac{C_{total} \times V}{S},$$

$$F_{re} = F_{total} - F_{atm},$$

Biogeosciences Discuss., https://doi.org/10.5194/bg-2018-258
Manuscript under review for journal Biogeosciences
Discussion started: 12 July 2018

Assuming F_{atm} was stable during the period until next observation (Δt), we can obtain the annual export flux of unprocessed $NO_3^-{}_{atm}$ per unit area of the catchment (M_{atm}) by integrating the F_{atm} values for each year of observation using equation (6).

$$M_{atm} = \sum(F_{atm}(t) \times \Delta t),$$

We can also obtain the annual export flux for NO_3^- (M_{total}) and $NO_3^-{}_{re}$ (M_{re}) by integrating F_{total} and F_{re} for each year of observation using equations (7) and (8).

$$M_{total} = \sum(F_{total}(t) \times \Delta t),$$

$$M_{re} = \sum(F_{re}(t) \times \Delta t),$$

By dividing M_{atm} by the deposition flux of $NO_3^-{}_{atm}$ per unit area of the catchment, we can estimate the portion of $NO_3^-{}_{atm}$ deposited onto the catchment area which survived biological processing in the catchment basin.

$$\frac{M_{atm}}{D_{atm}} = \frac{\sum(F_{atm}(t) \times \Delta t)}{D_{atm}},$$

where D_{atm} denotes the deposition flux of $NO_3^-{}_{atm}$ per unit area of the catchment.

3 Results

3.1 KJ site

The temporal variation in nitrate concentration and values of $\delta^{15}N$ and $\Delta^{17}O$ of nitrate in the stream water exported from the KJ site are presented in Fig. 3, together with the export fluxes of nitrate (F_{total}) and unprocessed $NO_3^-{}_{atm}$ (F_{atm}), on a logarithmic scale. The $\delta^{18}O$ values of nitrate in the stream and soil water samples are plotted as a function of $\Delta^{17}O$ in Fig. 4. Furthermore, the temporal variation in the concentration of nitrate in the soil and stream water is presented in Fig. 5 on a logarithmic scale.

We identified clear enrichment in the export fluxes of nitrate in stream water (F_{total}) in winter, with the maximum flux occurring around December every year (Fig. 3(d)). Similar nitrate enrichment in winter was found in previous studies undertaken between 2002 and 2007 on the same stream (Kamisako et al., 2008). In accordance with the increase in F_{total} in winter, F_{atm} also increased.

Biogeosciences Discuss., https://doi.org/10.5194/bg-2018-258
Manuscript under review for journal Biogeosciences
Discussion started: 12 July 2018

Continuous monitoring of $\Delta^{17}O$ (Tsunogai et al., 2014) and $\delta^{18}O$ (Kendall et al., 1995; Ohte et al., 2004; Pellerin et al., 2012; Piatek et al., 2005) of nitrate in past studies of streams eluted from forested catchments have often shown F_{atm} enrichment during spring, probably due to $NO_3^-{}_{atm}$ accumulated in the snowpack discharging to the streams. At the KJ site, however, we could not find significant enrichment of F_{atm} in spring.

The flux-weighted average stream nitrate concentration was 58.4 μmol L^{-1}. Compared to the average of 45.0 μmol L^{-1} determined during past observations (Kamisako et al., 2008), further enrichment of nitrate was found at the KJ site in this study. The stable isotopic composition of stream nitrate, differed from the concentration, showing only small temporal variation, from –3.2‰ to +1.6‰ for $\delta^{15}N$ (Fig. 3(b)), from –2.3‰ to +2.2‰ for $\delta^{18}O$ (Fig. 4), and from +0.8‰ to +2.0‰ for $\Delta^{17}O$ (Fig. 3(c)). The flux-weighted average for the $\delta^{15}N$, $\delta^{18}O$ and $\Delta^{17}O$ values of nitrate were –2.2‰, +0.50‰, and +1.49‰, respectively. These values are typical for nitrate exported from temperate forested watersheds (Bourgeois et al., 2018; Nakagawa et al., 2013; Riha et al., 2014; Sabo et al., 2016; Tsunogai et al., 2014; Tsunogai et al., 2016).

Compared with the stream water, the soil water displayed nitrate enrichment, up to 1.6 mmol L^{-1} or more (Fig. 5). The soil nitrate concentration showed significant seasonal variation, with the maximum occurring in summer (August to September) and minimum in winter (December) in our dataset (Fig. 5). Because we could not obtain data for soil water during January to March due to heavy snow on the site, much more nitrate depletion may have occurred during those months.

The stable oxygen isotopic compositions ($\delta^{18}O$ and $\Delta^{17}O$) of nitrate in the soil water also showed large seasonal variation, from –7.1‰ to +11.1‰ for $\delta^{18}O$, and from +0.1‰ to +5.7‰ for $\Delta^{17}O$ (Figs. 3(c) and 4), with the maximum occurring in winter and minimum in summer (Fig. 3(c)). The stable oxygen isotopic compositions ($\delta^{18}O$ and $\Delta^{17}O$) of nitrate showed a linear correlation on the $\Delta^{17}O$-$\delta^{18}O$ plot (Fig. 4). Because $NO_3^-{}_{atm}$ is enriched in both $\Delta^{17}O$ and $\delta^{18}O$ and is the only possible source of nitrate with $\Delta^{17}O$ values higher than 0‰, mixing ratios between $NO_3^-{}_{atm}$ and $NO_3^-{}_{re}$ were primarily responsible for the variation in both $\Delta^{17}O$ and $\delta^{18}O$ in the soil water nitrate (Costa et al., 2011). Moreover, the soil nitrate that was enriched during summer is mostly remineralized nitrate,

Biogeosciences Discuss., https://doi.org/10.5194/bg-2018-258
Manuscript under review for journal Biogeosciences
Discussion started: 12 July 2018

produced through nitrification in soils. The stable nitrogen isotopic composition ($\delta^{15}N$) of nitrate in the soil water samples also showed a larger temporal variation compared to the stream water nitrate, from –8.2‰ to +0.5‰ (Fig. 3(b)).

The areal bulk deposition flux of $NO_3^-{}_{atm}$ determined for the KJ site was 0.125 mmol m^{-2} day^{-1} (45.6 mmol m^{-2} yr^{-1}) on average during the observation period. This value almost corresponds with the average areal total (wet + dry) deposition flux of atmospheric nitrate determined at the nearby Sado-seki National Acid Rain Monitoring Station on Sado Island (38°14'59"N, 138°24'00"E; Fig. 1(a)) in 2013 (49.2 mmol m^{-2} yr^{-1}) and 2014 (48.3 mmol m^{-2} yr^{-1}). The monitoring values are the integrated values of the wet deposition flux of nitrate (30.6 and 27.1 mmol m^{-2} yr^{-1} in 2013 and 2014, respectively), dry deposition flux of gaseous HNO_3 (13.5 and 15.3 mmol m^{-2} yr^{-1} in 2013 and 2014, respectively), and dry deposition flux of particulate nitrate (5.1 and 5.9 mmol m^{-2} yr^{-1} in 2013 and 2014, respectively) (EANET, 2014, 2015).

As presented in section 2.4, the deposition flux could be either underestimated, due to insufficient inclusion of the dry deposition flux (Aikawa et al., 2003) or overestimated, due to the progress of nitrification in sample bottles during storage in the field until recovery (Clow et al., 2015). As a result, we use the bulk deposition flux determined in this study (45.6 mmol m^{-2} yr^{-1}) as the areal total (wet + dry) deposition flux of $NO_3^-{}_{atm}$ (D_{atm}) at the KJ site by allowing error range of 20% in the discussions in this study.

3.2 IJ1 and IJ2 sites

The temporal variation in the nitrate concentration and the values of $\delta^{15}N$ and $\Delta^{17}O$ of nitrate in the stream water from IJ1 and IJ2 is presented in Fig. 6, together with the export fluxes of nitrate (F_{total}) and unprocessed atmospheric nitrate (F_{atm}) at IJ1, on a logarithmic scale. The values ranged from 13.6 to 56.3 μmol L^{-1} for nitrate concentration (Fig. 6(a)), –2.2‰ to +5.0‰ for $\delta^{15}N$ (Fig. 6(b)), +1.0‰ to +9.8‰ for $\delta^{18}O$, and +0.7‰ to +2.8‰ for $\Delta^{17}O$ (Fig. 6(c)) in IJ1, and from 11.1 to 53.0 μmo l L^{-1} for nitrate concentration (Fig. 6(a)), –1.1‰ to +3.3‰ for $\delta^{15}N$ (Fig. 6(b)), -2.1‰ to +8.0‰ for $\delta^{18}O$, and +0.4‰ to +2.2‰ for $\Delta^{17}O$ (Fig. 6(c)) in IJ2.

Biogeosciences Discuss., https://doi.org/10.5194/bg-2018-258
Manuscript under review for journal Biogeosciences
Discussion started: 12 July 2018

Differing from the KJ site, we could not find any clear seasonal variation in the concentration of nitrate, the stable isotopic compositions of nitrate, or the export fluxes of nitrate (F_{total}) and $NO_3^-{}_{atm}$ (F_{atm}) in the stream water from IJ1 and IJ2. We could not identify a spring maximum in these catchments either. On the other hand, we did find sporadic, short-term increases in nitrate of about 40 μmol L^{-1} during the observation period. The increases were observed simultaneously at IJ1 and IJ2. Similar sporadic nitrate enrichment was found on Aug. 1994 during observations from 1988 to 2003 on the stream IJ1 (Nakahara et al., 2010). Except for the sporadic, short-term enrichment of nitrate, the stream water nitrate concentration and isotopic composition were almost constant at each site during the observation period. The flux-weighted average for the $\delta^{15}N$, $\delta^{18}O$ and $\Delta^{17}O$ values of stream nitrate were +0.23‰, +3.76‰, and +1.50‰ at IJ1, respectively, and +0.42‰, +1.57‰, and +0.85‰ at IJ2, respectively. These values are typical for nitrate exported from temperate forested watersheds (Bourgeois et al., 2018; Nakagawa et al., 2013; Riha et al., 2014; Sabo et al., 2016; Tsunogai et al., 2014; Tsunogai et al., 2016).

One of the striking features of the stream nitrate concentration at these sites was nitrate enrichment of about 7±5 μmol L^{-1} in IJ1 compared to IJ2 throughout the observation period. Amongst the 39 pairs of data points, the reverse relationship (nitrate depletion in IJ1 compared with IJ2) was found only three times (Aug. 2012, July 2013, and Aug. 2013). Even during the sporadic, short-term increases in nitrate, the nitrate concentrations in IJ1 were generally higher than IJ2. Furthermore, not only the stream nitrate concentration but also the $\Delta^{17}O$ values of nitrate in IJ1 were higher compared to IJ2 (Fig. 6(c)). Amongst the 39 pairs of data points, the reverse relationship (lower $\Delta^{17}O$ values of nitrate in IJ1 compared with IJ2) was found only five times.

The flux-weighted average stream nitrate concentrations during the observation period were 24.4 and 17.1 μmol L^{-1} in IJ1 and IJ2, respectively. While the stream nitrate concentration in IJ1 showed an increasing trend year to year, from 22 μmol L^{-1} in the late 1980s to 42 μmol L^{-1} in the early 2000s (Nakahara et al., 2010), the present study revealed that the trend in stream nitrate concentration has changed from increasing to decreasing, probably since the 2000s.

Biogeosciences Discuss., https://doi.org/10.5194/bg-2018-258
Manuscript under review for journal Biogeosciences
Discussion started: 12 July 2018

The areal deposition flux of $NO_3^-{}_{atm}$ was 0.122 mmol m^{-2} day^{-1} (44.5 mmol m^{-2} yr^{-1}) on average during the observation period (EANET, 2014, 2015). This value almost corresponds with the observed value from the KJ monitoring site.

4 Discussion

4.1 Origin of stream nitrate in KJ site

The runoff paths of water from the forested slope to the stream can be classified into (1) overland flow, (2) through flow (shallow subsurface flow above the water table), and (3) groundwater flow (movement through the saturated zone) (Berner and Berner, 1987). The $\Delta^{17}O$ values of stream nitrate (+0.8 to 2.0‰) indicated that the major portion of stream nitrate was remineralized nitrate ($NO_3^-{}_{re}$), produced through nitrification in soils, and thus unprocessed atmospheric nitrate ($NO_3^-{}_{atm}$) contributed a minor portion of the total nitrate. This means that nitrate supplied via overland flow was a minor portion of stream nitrate. While stream nitrate showed similar $\Delta^{17}O$ values to soil nitrate, the variation in stream nitrate was much smaller than soil nitrate (Fig. 4); from +0.8 to +2.0‰ for stream nitrate, while from +0.1‰ to +5.7‰ for soil nitrate. Because $\Delta^{17}O$ is stable during partial metabolism in soils (such as assimilation and denitrification), the present results imply that nitrate in the catchment groundwater was the major source of stream nitrate, while through flow was a minor contributor of nitrate. That is, while the $\Delta^{17}O$ values of soil nitrate represented the original $\Delta^{17}O$ values of nitrate in the groundwater, the large variation in the $\Delta^{17}O$ values of soil nitrate was buffered by huge nitrate reserves in the groundwater (Kabeya et al., 2007; Tsunogai et al., 2016). Therefore, little seasonal variation in the $\Delta^{17}O$ values of stream nitrate and only small enrichment of F_{atm} during spring were observed.

This hypothesis was supported by the $\delta^{18}O$ values of nitrate. While the $\delta^{18}O$ values of nitrate could change during partial metabolism, the range of $\delta^{18}O$ variation in stream nitrate (-2.3 to +2.2‰) was within the range of soil nitrate (-7.1 to +11.1‰) (Fig. 4). In addition, stream nitrate data plotted along the hypothetical mixing line between $NO_3^-{}_{atm}$ and $NO_3^-{}_{re}$ for soil nitrate (Fig. 4). We

concluded that soil nitrate was the primary source of stream nitrate but had been buffered by the huge nitrate reserve in the groundwater.

By extrapolating the linear correlation between $\Delta^{17}O$ and $\delta^{18}O$ to $\Delta^{17}O$ = 0‰, we obtained the $\delta^{18}O$ value of −2.7±0.6 ‰ as the average $\delta^{18}O$ value of $NO_3^-{}_{re}$ in both stream and soil water. The $\delta^{18}O$ value of $NO_3^-{}_{re}$ correlated strongly with that of $NO_3^-{}_{re}$ being exported from forested catchments, for example $NO_3^-{}_{re}$ exported from cool-temperate forested watersheds in Rishiri Island ($\delta^{18}O$ = −4.2±2.4‰), where the $\delta^{18}O(H_2O)$ was around −13‰ (Tsunogai et al., 2010), $NO_3^-{}_{re}$ exported from a cool-temperate forested catchment in Teshio ($\delta^{18}O$ = −3.6±0.7‰), where the $\delta^{18}O(H_2O)$ was around −11‰ (Tsunogai et al., 2014), and $NO_3^-{}_{re}$ exported from the temperate forested watersheds around Lake Biwa ($\delta^{18}O$ = −2.9±1.2‰), where the $\delta^{18}O(H_2O)$ was −7.8±1.0‰ (Tsunogai et al., 2016).

The possible $\delta^{18}O$ value of $NO_3^-{}_{re}$ produced through microbial nitrification under an H_2O of −9.1‰ (the average $\delta^{18}O$ value of H_2O in the stream water samples) is −5.7±2.0‰ (Buchwald et al., 2012). Because the partial metabolism of nitrate would enhance the $\delta^{18}O$ values of residual nitrate to some extent, the observed low $\delta^{18}O$ value (−2.7±0.6 ‰), which is close to the original $\delta^{18}O$ value of $NO_3^-{}_{re}$ in both the stream and soil water, implies that partial metabolism subsequent to the production of $NO_3^-{}_{re}$ was minor in the forested soils in KJ. The relationship between $\Delta^{17}O$ and $\delta^{18}O$ of nitrate shown in Fig. 4 is highly useful for determining the $\delta^{18}O$ value of $NO_3^-{}_{re}$ in each catchment and thus the behaviour of produced $NO_3^-{}_{re}$ within the catchment (Tsunogai et al., 2010).

4.2 Seasonal variation in the KJ site

Nitrate in the KJ site presented clear export flux (F_{total}) enrichment in winter (Fig. 3(d)). High precipitation in winter is partially responsible for the enhancement of the export flux of water and thus F_{total} enrichment in winter. However, it is difficult to explain a nitrate concentration enrichment of more than 80 μmol L^{-1} only by higher precipitation in winter. Kamisako et al. (2008) found the same trend during their observation period from 2002 to 2007 at the same site, and proposed that active biological assimilation of nitrate during the growing season was responsible for nitrate

Biogeosciences Discuss., https://doi.org/10.5194/bg-2018-258
Manuscript under review for journal Biogeosciences
Discussion started: 12 July 2018

depletion in summer, and thus enrichment in winter. However, the present study revealed that the soil nitrate showed the opposite trend: nitrate-enrichment in summer and depletion in winter, probably due to active nitrification in the soil in summer (Breuer et al., 2002; Hoyle et al., 2006; Tsunogai et al., 2014; Zaman and Chang, 2004). A clear decrease in the $\Delta^{17}O$ values of soil nitrate in summer (Fig. 3(c)) also supports active nitrification in summer (Tsunogai et al., 2014), because the $\Delta^{17}O$ values of remineralized nitrate produced through nitrification are 0‰. Moreover, if such biological assimilation was responsible for the nitrate depletion in summer, significant enrichment in the values of $\delta^{15}N$ and $\delta^{18}O$ could be expected in the residual portion of nitrate exported into the stream, while we could not find such enrichment in summer (Figs. 3 and 4). As a result, it is difficult to assume active biological assimilation of nitrate in summer as responsible for the seasonal variation in stream nitrate concentration.

As presented in section 4.1, the major source of stream nitrate is likely groundwater nitrate which has been recharged by soil nitrate. The residence time of groundwater was estimated to be a few months for most of the catchments in Japan with a humid temperate climate using the deuterium excess as a tracer (Kabeya et al., 2007; Takimoto et al., 1994). While the soil nitrate showed nitrate-enrichment in summer and depletion in winter, stream nitrate samples taken at the same time showed the opposite trend (Fig. 7). However, if we assume a time lag of four months between the samples, as presented in Fig. 7, stream nitrate shows a normal correlation with soil nitrate ($r^2 = 0.41$ and $p < 0.03$ for SLS20, $r^2 = 0.37$ and $p < 0.03$ for SMS20).

The small increase/decrease in the $\Delta^{17}O$ values of stream nitrate can be explained by the increase/decrease in the $\Delta^{17}O$ values of soil nitrate four months earlier. This delay time reflects the magnitude of the nitrate reservoir in the groundwater of this catchment. We concluded that active nitrification in summer was largely responsible for stream nitrate enrichment in winter, by increasing the nitrate concentration in groundwater that reflects nitrate accumulation over a few months prior to the observation.

Biogeosciences Discuss., https://doi.org/10.5194/bg-2018-258
Manuscript under review for journal Biogeosciences
Discussion started: 12 July 2018

4.3 The export flux of atmospheric nitrate and the relationship with nitrogen saturation

As already implied in previous studies at the KJ site (Kamisako et al., 2008; Sase et al., 2015), stream nitrate at the KJ site is characterized by nitrate enrichment. The flux-weighted annual average stream nitrate concentration determined in this study was 58.4 μmol L^{-1} at the KJ site, and 24.4 and 17.1 μmol L^{-1} at the IJ1 and IJ2 sites, respectively. The annual export flux of nitrate per unit area of the catchment (M_{total}) from the KJ site (158 mmol m^{-2}) was also higher than the fluxes from the IJ1 and IJ2 sites (64 and 43 mmol m^{-2}, respectively). In accordance with the variation in the export flux of nitrate, the unprocessed $NO_3^-{}_{atm}$ per unit area of the catchment (M_{atm}) also varied: 8.8 (mmol m^{-2}) from KJ, 5.7 (mmol m^{-2}) from IJ1, and 2.3 (mmol m^{-2}) from IJ2. As a result, not only the export flux of $NO_3^-{}_{re}$ produced through nitrification in forested soils but also the direct drainage flux of unprocessed $NO_3^-{}_{atm}$ increased in accordance with the increases in the export flux of nitrate between the catchments.

Because the differences in the deposition flux of $NO_3^-{}_{atm}$ (D_{atm}) were small between the studied catchments, regional changes in D_{atm} cannot be the direct cause of the observed variation in M_{atm} in accordance with variation in the stream nitrate concentrations. Moreover, the M_{atm}/D_{atm} ratios estimated using the equation (9) also varied in accordance with the stream nitrate concentrations (Fig. 8(a)): 9.4±2.6% at the KJ site, 6.5±1.8% at the IJ1 site, and 2.6±0.6% at the IJ2 site, and thus the residual portion (90.6±2.6% in KJ, 93.5±1.8% in IJ1, and 97.4±0.6% in IJ2) underwent biological processing (such as assimilation and denitrification) before being exported from the surface ecosystem. The normal correlation between stream nitrate concentrations and the M_{atm}/D_{atm} ratios is an important finding to interpret the changes in stream nitrate concentrations between the catchments.

Rose et al. (2015a) determined M_{atm} in forested catchments under different nitrogen saturation stages and found similar M_{atm} variation in accordance with stream nitrate concentrations. When we estimated M_{atm}/D_{atm} ratios for the catchments studied in Rose et al. (2015a) and plotted them as a function of the stream nitrate concentration in Fig. 8(a) together with our data, both results plotted on the same region, showing a clear increasing trend in the M_{atm}/D_{atm} ratios in accordance with

increases in the stream nitrate concentration and thus increases in the stage of nitrogen saturation (Fig. 8(a)).

Either increased nitrification rates in forested soils or reductions in the N retention ability are assumed to be responsible for enhanced nitrogen leaching from soils and the increased export flux of nitrate in nitrogen-saturated catchments (Peterjohn et al., 1996). In the studied catchments, however, it is not possible to explain the variation in the export flux of unprocessed $NO_3^-{}_{atm}$ between the catchments only by the variation in the nitrification rates in forested soils, because M_{atm}/D_{atm} ratios are stable during the progress of nitrification in forested soils (Fig. 9). Rather, varying N retention abilities (varying biological assimilation rates of nitrate, especially) in forested soils must be needed to explain the observed variation in the stream nitrate concentration and M_{atm}/D_{atm} ratios between the catchments simultaneously (Fig. 9).

The present results imply that the major impact of nitrogen saturation was on the biological assimilation processes of nitrate, rather than the biological nitrification processes in soils. Besides, the M_{atm}/D_{atm} ratio in each forested catchment can be used as an index for the nitrogen saturation stage. That is, the studied catchments were under nitrogen saturation in the stage order of KJ > IJ1 > IJ2 (Fig. 8(a)).

All nitrate other than unprocessed $NO_3^-{}_{atm}$ can be classified as $NO_3^-{}_{re}$, including nitrate produced through natural or anthropogenic processes in the biosphere, hydrosphere, and geosphere, and nitrate stored in soil, fertilizer, manure, and sewage. Therefore, stream nitrate enrichment due to artificial processes does not increase M_{atm}/D_{atm} ratios. As a result, the M_{atm}/D_{atm} ratio in each forested catchment can be used as an index to differentiate stream nitrate enrichment due to nitrogen saturation, from stream nitrate enrichment due to artificial processes.

Stoddard (1994) proposed the disappearance of seasonality in stream nitrate concentrations as an index for nitrogen saturation in forest ecosystems. However, because the seasonal changes in forested soils are buffered by groundwater in humid temperate climates such as Japan, the seasonality in stream nitrate concentrations is not clear even when exported from “normal” forest (i.e., forest under stage zero of nitrogen saturation) (Mitchell et al., 1997). As a result, seasonality is

not a reliable index of nitrogen saturation in forests in humid temperate climates. The present study implies that the M_{atm}/D_{atm} ratio in each forested catchment, estimated from ^{17}O-excess of stream nitrate, can be a robust, alternative index for the stage of nitrogen saturation irrespective of the humidity of the climate.

To estimate M_{atm}/D_{atm} ratios in a catchment, the export flux of nitrate (M_{total}), the ^{17}O-excess of stream nitrate, and the deposition rate of $NO_3^-{}_{atm}$ (D_{atm}) must be estimated. The deposition rate of $NO_3^-{}_{atm}$ (D_{atm}), however, is a difficult parameter to determine in forested catchments in general. An alternative parameter which we can determine more easily is the average concentration of $NO_3^-{}_{atm}$ in stream water (C_{atm}), so we plotted C_{atm} as a function of the average concentration of nitrate (C_{total}) in Fig. 8(b). While the correlation coefficient was poorer than the M_{atm}/D_{atm} ratio, C_{atm} also presented a normal correlation with the concentration of stream nitrate (Fig. 8(b)), probably because the differences in (1) $NO_3^-{}_{atm}$ concentration in wet deposition, (2) the dry deposition flux of $NO_3^-{}_{atm}$, and (3) the evaporative loss flux of water deposited onto forested soils were small within the catchments. As a result, in forested catchments where we can assume the differences in (1), (2), and (3) from the studied catchments are minimal, we can use C_{atm} as an alternative but less reliable index of the stage of nitrogen saturation instead of M_{atm}/D_{atm} ratios.

Previous studies also found that the relative mixing ratios of unprocessed $NO_3^-{}_{atm}$ to total nitrate (M_{atm}/M_{total} ratios) increased in proportion to the extent of both forest decline (Durka et al., 1994) and strip-cutting (Tsunogai et al., 2014). In the present study, however, we could not find clear changes in the M_{atm}/M_{total} ratios between the catchments: 5.6% for the KJ site, 5.7% for the IJ1 site, and 3.3% for the IJ2 site. Rose et al. (2015a) also reported that the M_{atm}/M_{total} ratios were almost the same between forested catchments irrespective of changes in their nitrogen saturation stages. While the annual export flux of nitrate and $NO_3^-{}_{atm}$ per unit area of the catchment increased by 6 and 20 times in accordance with strip-cutting (Tsunogai et al., 2014), increases in M_{total} and M_{atm} in KJ compared to IJ2 were only 3 and 4 times, respectively, so we could not find clear changes in M_{atm}/M_{total} ratios between the catchments. Even in forested catchments where it is difficult to

determine D_{atm}, the M_{atm}/M_{total} ratio is not a suitable alternative index to the M_{atm}/D_{atm} ratio for the stages of nitrogen saturation.

5 Concluding remarks

By using the ^{17}O-excess of nitrate as a tracer, we clarified that the major source of nitrate in stream water eluted from the studied forested catchments was nitrate in groundwater. The present results imply that nitrate in groundwater is the major source of nitrate in stream water eluted from forested catchments in humid temperate climates. Moreover, we clarified that the seasonal variation in the concentrations of soil water nitrate was buffered by groundwater. As a result, caution is needed to clarify the causes of seasonal variations in chemical/isotopic compositions of stream water, because a time-lag from variations in soil water can be anticipated.

The export flux of unprocessed atmospheric nitrate relative to the deposition flux (M_{atm}/D_{atm} ratio) showed clear normal correlation with the flux-weighted average concentration of stream nitrate, not only in the forested catchments studied in this paper but also in all forested catchments studied using the ^{17}O-excess of nitrate as a tracer. As a result, reductions in the biological assimilation rates of nitrate in forested soils, rather than increased nitrification rates in forested soils, are largely responsible for the enrichment of stream nitrate due to nitrogen saturation. Furthermore, the export flux of unprocessed atmospheric nitrate relative to the deposition flux in each forested catchment is applicable as a new index of nitrogen saturation. Further studies are needed for stream nitrate exported from various forested catchments around the world to verify the present results, using the ^{17}O-excess of nitrate as a tracer of the unprocessed atmospheric nitrate in stream nitrate.

Acknowledgments

The samples analyzed in this study were colleted through the Long-term Monitoring of Transboundary Air Pollution and Acid Deposition by the Ministry of the Environment in Japan. We thank Ayaka Ikegami for drawing color altitude maps of the studied sites and Masanori Ito, Kosuke

Ikeya, Koji Takahashi, Takuya Ohyama, Shuichi Hara, Toshiyuki Matsushita, Takanori Miyauchi, Yoshiumi Matsumoto, Rei Nakane, Lin Cheng, and the other present/past members of the Biogeochemistry Group at Nagoya University for their valuable support during this study. This work was supported by a Grant-in-Aid for Scientific Research from the Ministry of Education, Culture, Sports, Science, and Technology of Japan under grant numbers 15H02804, 16K14308, 15K12187, 17H00780, 26241006, and 24651002.

References

Aber, J. D., Nadelhoffer, K. J., Steudler, P., and Melillo, J. M.: Nitrogen Saturation in Northern Forest Ecosystems Bioscience, 39, 378-386, 1989.

Aikawa, M., Hiraki, T., Tamaki, M., and Shoga, M.: Difference between filtering-type bulk and wet-only data sets based on site classification, Atmos. Environ., 37, 2597–2603, 2003.

Alexander, B., Hastings, M. G., Allman, D. J., Dachs, J., Thornton, J. A., and Kunasek, S. A.: Quantifying atmospheric nitrate formation pathways based on a global model of the oxygen isotopic composition ($\Delta^{17}O$) of atmospheric nitrate, Atmos. Chem. Phys., 9, 5043-5056, 2009.

Berner, E. K. and Berner, R. A.: The global water cycle: geochemistry and environment, Englewood Cliffs, N.J., Prentice-Hall, 1987.

Bourgeois, I., Savarino, J., Némery, J., Caillon, N., Albertin, S., Delbart, F., Voisin, D., and Clément, J.-C.: Atmospheric nitrate export in streams along a montane to urban gradient, Science of The Total Environment, 633, 329-340, 2018.

Breuer, L., Kiese, R., and Butterbach-Bahl, K.: Temperature and moisture effects on nitrification rates in tropical rain-forest soils, Soil Sci. Soc. Am. J., 66, 834-844, 2002.

Buchwald, C., Santoro, A. E., McIlvin, M. R., and Casciotti, K. L.: Oxygen isotopic composition of nitrate and nitrite produced by nitrifying cocultures and natural marine assemblages, Limnol. Oceanogr., 57, 1361-1375, 2012.

Clow, D. W., Roop, H. A., Nanus, L., Fenn, M. E., and Sexstone, G. A.: Spatial patterns of atmospheric deposition of nitrogen and sulfur using ion-exchange resin collectors in Rocky Mountain National Park, USA, Atmos. Environ., 101, 149-157, 2015.

Dejwakh, N. R., Meixner, T., Michalski, G., and McIntosh, J.: Using ^{17}O to investigate nitrate sources and sinks in a semi-arid groundwater system, Environ. Sci. Technol., 46, 745-751, 2012.

Durka, W., Schulze, E.-D., Gebauer, G., and Voerkeliust, S.: Effects of forest decline on uptake and leaching of deposited nitrate determined from ^{15}N and ^{18}O measurements, Nature, 372, 765 - 767, 1994.

EANET: Data Report 2013, Network center for EANET (Acid Deposition Monitoring Network in East Asia), Nigata, Japan, 2014.

EANET: Data Report 2014, Network center for EANET (Acid Deposition Monitoring Network in East Asia), Nigata, Japan, 2015.

Hirota, A., Tsunogai, U., Komatsu, D. D., and Nakagawa, F.: Simultaneous determination of $\delta^{15}N$ and $\delta^{18}O$ of N_2O and $\delta^{13}C$ of CH_4 in nanomolar quantities from a single water sample, Rapid Commun. Mass Spectrom., 24, 1085-1092, 2010.

Hoyle, F. C., Murphy, D. V., and Fillery, I. R. P.: Temperature and stubble management influence microbial CO_2-C evolution and gross N transformation rates, Soil Biology and Biochemistry, 38, 71-80, 2006.

Kabeya, N., Katsuyama, M., Kawasaki, M., Ohte, N., and Sugimoto, A.: Estimation of mean residence times of subsurface waters using seasonal variation in deuterium excess in a small headwater catchment in Japan, Hydrol. Process., 21, 308-322, 2007.

Kaiser, J., Hastings, M. G., Houlton, B. Z., Röckmann, T., and Sigman, D. M.: Triple oxygen isotope analysis of nitrate using the denitrifier method and thermal decomposition of N_2O, Anal. Chem., 79, 599-607, 2007.

Kamisako, M., Sase, H., Matsui, T., Suzuki, H., Takahashi, A., Oida, T., Nakata, M., Totsuka, T., and Ueda, H.: Seasonal and annual fluxes of inorganic constituents in a small catchment of a Japanese cedar forest near the Sea of Japan, Water Air Soil Poll., 195, 51-61, 2008.

Kendall, C.: Tracing Nitrogen Sources and Cycling in Catchments. In: Isotope Tracers in Catchment Hydrology, Kendall, C. and McDonnell, J. J. (Eds.), Elsevier Science B.V., Amsterdam, 839 p., Amsterdam, 1998.

Kendall, C., Campbell, D. H., Burns, D. A., Schanley, J. B., Silva, S. R., and Chang, C. C. Y.: Tracing sources of nitrate in snowmelt runoff using the oxygen and nitrogen isotopic compositions of nitrate. In: Biogeochemistry of seasonally snow-covered catchments, Proceedings of a Boulder Symposium, IAHS Publication, 1995.

Komatsu, D. D., Ishimura, T., Nakagawa, F., and Tsunogai, U.: Determination of the $^{15}N/^{14}N$, $^{17}O/^{16}O$, and $^{18}O/^{16}O$ ratios of nitrous oxide by using continuous-flow isotope-ratio mass spectrometry, Rapid Commun. Mass Spectrom., 22, 1587-1596, 2008.

Konno, U., Tsunogai, U., Komatsu, D. D., Daita, S., Nakagawa, F., A.Tsuda, Matsui, T., Eum, Y.-J., and Suzuki, K.: Determination of total N_2 fixation rates in the ocean taking into account both the particulate and filtrate fractions, Biogeosciences, 7, 2369-2377, doi:10.5194/bg-7-2369-2010, 2010.

Liu, T., Wang, F., Michalski, G., Xia, X., and Liu, S.: Using N-15, O-17, and O-18 To Determine Nitrate Sources in the Yellow River, China, Environmental Science & Technology, 47, 2013.

McIlvin, M. R. and Altabet, M. A.: Chemical conversion of nitrate and nitrite to nitrous oxide for nitrogen and oxygen isotope analysis in freshwater and seawater, Anal. Chem., 77, 5589-5595, 2005.

McIsaac, G. F., David, M. B., Gertner, G. Z., and Goolsby, D. A.: Eutrophication: Nitrate flux in the Mississippi River, Nature, 414, 166-167, 2001.

Michalski, G., Meixner, T., Fenn, M., Hernandez, L., Sirulnik, A., Allen, E., and Thiemens, M.: Tracing Atmospheric Nitrate Deposition in a Complex Semiarid Ecosystem Using $\Delta^{17}O$, Environ. Sci. Technol., 38, 2175-2181, 2004.

Michalski, G., Savarino, J., Böhlke, J. K., and Thiemens, M.: Determination of the total oxygen isotopic composition of nitrate and the calibration of a $\Delta^{17}O$ nitrate reference material, Anal. Chem., 74, 4989-4993, 2002.

Michalski, G., Scott, Z., Kabiling, M., and Thiemens, M. H.: First measurements and modeling of $\Delta^{17}O$ in atmospheric nitrate, Geophys. Res. Lett., 30, doi:10.1029/2003GL017015, 2003.

Miller, M. F.: Isotopic fractionation and the quantification of ^{17}O anomalies in the oxygen three-isotope system: an appraisal and geochemical significance, Geochim. Cosmochim. Acta, 66, 1881-1889, 2002.

Mitchell, M. J., Iwatsubo, G., Ohrui, K., and Nakagawa, Y.: Nitrogen saturation in Japanese forests: an evaluation, Forest Ecol. Manag., 97, 39-51, 1997.

Morin, S., Savarino, J., Frey, M. M., Domine, F., Jacobi, H. W., Kaleschke, L., and Martins, J. M. F.: Comprehensive isotopic composition of atmospheric nitrate in the Atlantic Ocean boundary layer from 65°S to 79°N, J. Geophys. Res., 114, doi:10.1029/2008jd010696, 2009.

Morin, S., Savarino, J., Frey, M. M., Yan, N., Bekki, S., Bottenheim, J. W., and Martins, J. M. F.: Tracing the origin and fate of NOX in the Arctic atmosphere using stable isotopes in nitrate, Science, 322, 730-732, 2008.

Nakagawa, F., Suzuki, A., Daita, S., Ohyama, T., Komatsu, D. D., and Tsunogai, U.: Tracing atmospheric nitrate in groundwater using triple oxygen isotopes: Evaluation based on bottled drinking water, Biogeosciences, 10, 3547-3558, 2013.

Nakahara, O., Takahashi, M., Sase, H., Yamada, T., Matsuda, K., Ohizumi, T., Fukuhara, H., Inoue, T., Takahashi, A., Kobayashi, H., Hatano, R., and Hakamata, T.: Soil and stream water acidification in a forested catchment in central Japan, Biogeochemistry, 97, 141-158, 2010.

Nelson, D. M., Tsunogai, U., Dong, D., Ohyama, T., Komatsu, D. D., Nakagawa, F., Noguchi, I., and Yamaguchi, T.: Triple oxygen isotopes indicate urbanization affects sources of nitrate in wet and dry atmospheric deposition, Atmos. Chem. Phys., 18, 6381-6392, 2018.

Ohte, N., Sebestyen, S. D., Shanley, J. B., Doctor, D. H., Kendall, C., Wankel, S. D., and Boyer, E. W.: Tracing sources of nitrate in snowmelt runoff using a high-resolution isotopic technique, Geophys. Res. Lett., 31, doi:10.1029/2004GL020908, 2004.

Paerl, H. W.: Controlling eutrophication along the freshwater–marine continuum: Dual nutrient (N and P) reductions are essential, Estuar. Coasts, 32, 593-601, 2009.

Pellerin, B., Saraceno, J., Shanley, J., Sebestyen, S., Aiken, G., Wollheim, W., and Bergamaschi, B.: Taking the pulse of snowmelt: in situ sensors reveal seasonal, event and diurnal patterns of nitrate and dissolved organic matter variability in an upland forest stream, Biogeochemistry, 108, 183-198, 2012.

Peterjohn, W. T., Adams, M. B., and Gilliam, F. S.: Symptoms of nitrogen saturation in two central Appalachian hardwood forest ecosystems, Biogeochemistry, 35, 507–522, 1996.

Piatek, K. B., Mitchell, M. J., Silva, S. R., and Kendall, C.: Sources of nitrate in snowmelt discharge: evidence from water chemistry and stable isotopes of nitrate, Water Air Soil Poll., 165, 13-35, 2005.

Riha, K. M., Michalski, G., Gallo, E. L., Lohse, K. A., Brooks, P. D., and Meixner, T.: High Atmospheric Nitrate Inputs and Nitrogen Turnover in Semi-arid Urban Catchments, Ecosystems, 17, 1309-1325, 2014.

Rose, L. A., Elliott, E. M., and Adams, M. B.: Triple Nitrate Isotopes Indicate Differing Nitrate Source Contributions to Streams Across a Nitrogen Saturation Gradient, Ecosystems, 18, 1209-1223, 2015a.

Rose, L. A., Sebestyen, S. D., Elliott, E. M., and Koba, K.: Drivers of atmospheric nitrate processing and export in forested catchments, Water Resour. Res., 51, 1333-1352, 2015b.

Sabo, R. D., Nelson, D. M., and Eshleman, K. N.: Episodic, seasonal, and annual export of atmospheric and microbial nitrate from a temperate forest, Geophys. Res. Lett., 43, 683-691, 10.1002/2015GL066758, 2016.

Sase, H., Matsuda, K., Visaratana, T., Garivait, H., Yamashita, N., Kietvuttinon, B., Hongthong, B., Luangjame, J., Khummongkol, P., Shindo, J., Endo, T., Sato, K., Uchiyama, S., Miyazawa, M.,

Nakata, M., and Lenggoro, I. W.: Deposition Process of Sulfate and Elemental Carbon in Japanese and Thai Forests, Asian Journal of Atmospheric Environment, 6, 246-258, 2012.

Sase, H., Ohizumi, T., Yamashita, N., Visaratana, T., Kietvuttinon, B., Garivait, H., and Majid, N. M.: Dynamics of Sulphur Derived from Atmospheric Deposition and its Possible Impacts on East Asian Forests: Final Report Submitted to APN (Project Refence Number: ARCP2013-13CMY-Sase), Asia-Pacific Network for Global Change Research, Kobe, Japan, 2015.

Sase, H., Takahashi, A., Sato, M., Kobayashi, H., Nakata, M., and Totsuka, T.: Seasonal variation in the atmospheric deposition of inorganic constituents and canopy interactions in a Japanese cedar forest, Environmental Pollution, 152, 1-10, 2008.

Stoddard, J. L.: Long-Term Changes in Watershed Retention of Nitrogen: Its Causes and Aquatic Consequences. In: Environmental Chemistry of Lakes and Reservoirs, Baker, L. A. (Ed.), Advances in Chemistry Series, American Chemical Society, Washington DC, 1994.

Takagi, K., Fukuzawa, K., Liang, N., Kayama, M., Nomura, M., Hojyo, H., Sugata, S., Shibata, H., Fukazawa, T., Takahashi, Y., Nakaji, T., Oguma, H., Mano, M., Akibayashi, Y., Murayama, T., Koike, T., Sasa, K., and Fujinuma, Y.: Change in CO_2 balance under a series of forestry activities in a cool-temperate mixed forest with dense undergrowth, Global Change Biology, 15, 1275–1288, 2009.

Takimoto, H., Tanaka, T., and Horino, H.: Does forest conserve runoff discharge during drought?, Trans. Jpn. Soc. Irrig. Drain. Reclam. Eng., 170, 75-81, doi:10.11408/jsidre1965.1994.170_75, 1994 (in Japanese with English abstract).

Thiemens, M. H., Savarino, J., Farquhar, J., and Bao, H.: Mass-Independent Isotopic Compositions in Terrestrial and Extraterrestrial Solids and Their Applications, Acc. Chem. Res., 34, 645–652, 2001.

Tsunogai, U., Daita, S., Komatsu, D. D., Nakagawa, F., and Tanaka, A.: Quantifying nitrate dynamics in an oligotrophic lake using $\Delta^{17}O$, Biogeosciences, 8, 687-702, 2011.

Tsunogai, U., Kido, T., Hirota, A., Ohkubo, S. B., Komatsu, D. D., and Nakagawa, F.: Sensitive determinations of stable nitrogen isotopic composition of organic nitrogen through chemical conversion into N_2O, Rapid Commun. Mass Spectrom., 22, 345-354, 2008.

Tsunogai, U., Komatsu, D. D., Daita, S., Kazemi, G. A., Nakagawa, F., Noguchi, I., and Zhang, J.: Tracing the fate of atmospheric nitrate deposited onto a forest ecosystem in eastern Asia using $\Delta^{17}O$, Atmos. Chem. Phys., 10, 1809-1820, 2010.

Tsunogai, U., Komatsu, D. D., Ohyama, T., Suzuki, A., Nakagawa, F., Noguchi, I., Takagi, K., Nomura, M., Fukuzawa, K., and Shibata, H.: Quantifying the effects of clear-cutting and strip-cutting on nitrate dynamics in a forested watershed using triple oxygen isotopes as tracers, Biogeosciences, 11, 5411-5424, 2014.

Tsunogai, U., Miyauchi, T., Ohyama, T., Komatsu, D. D., Ito, M., and Nakagawa, F.: Quantifying nitrate dynamics in a mesotrophic lake using triple oxygen isotopes as tracers, Limnol. Oceanogr., 63, S458–S476, 2018.

Tsunogai, U., Miyauchi, T., Ohyama, T., Komatsu, D. D., Nakagawa, F., Obata, Y., Sato, K., and Ohizumi, T.: Accurate and precise quantification of atmospheric nitrate in streams draining land of various uses by using triple oxygen isotopes as tracers, Biogeosciences, 13, 3441-3459, 2016.

Wright, R. F. and Tietema, A.: Ecosystem response to 9 years of nitrogen addition at Sogndal, Norway, Forest Ecol. Manag., 71, 133-142, 1995.

Yamada, T., Inoue, T., Fukuhara, H., Nakahara, O., Izuta, T., Suda, R., Takahashi, M., Sase, H., Takahashi, A., Kobayashi, H., Ohizumi, T., and Hakamata, T.: Long-term Trends in Surface Water Quality of Five Lakes in Japan, Water, Air, and Soil Pollution: Focus, 7, 259-266, 2007.

Yamazaki, A., Watanabe, T., and Tsunogai, U.: Nitrogen isotopes of organic nitrogen in reef coral skeletons as a proxy of tropical nutrient dynamics, Geophys. Res. Lett., 38, doi:10.1029/2011GL049053, 2011.

Zaman, M. and Chang, S. X.: Substrate type, temperature, and moisture content affect gross and net N mineralization and nitrification rates in agroforestry systems, Biol. Fertil. Soils, 39, 269-279, 2004.

Biogeosciences Discuss., https://doi.org/10.5194/bg-2018-258
Manuscript under review for journal Biogeosciences
Discussion started: 12 July 2018

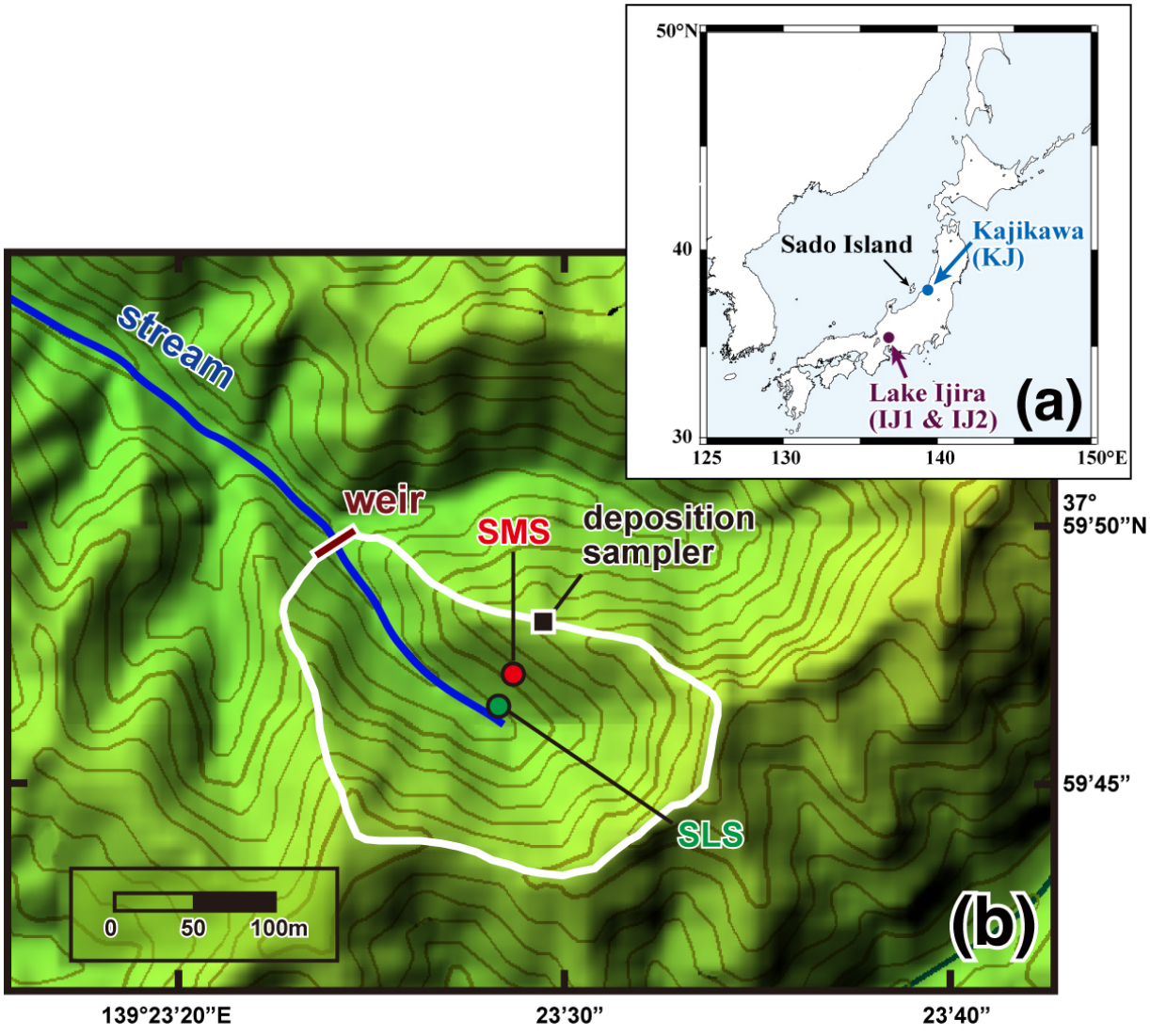

Figure 1: A map showing the locations of the studied watersheds (Kajikawa and Lake Ijira) in Japan (a), and a color altitude map of the KJ site (b), together with both the catchment area, shown by a white line, and the stream water sampling point, shown by a brown bar (weir). The green and red circles denote the locations of soil water sampling (SLS and SMS, respectively) and the black square denotes the location where the deposition sampler was set.

Biogeosciences Discuss., https://doi.org/10.5194/bg-2018-258
Manuscript under review for journal Biogeosciences
Discussion started: 12 July 2018

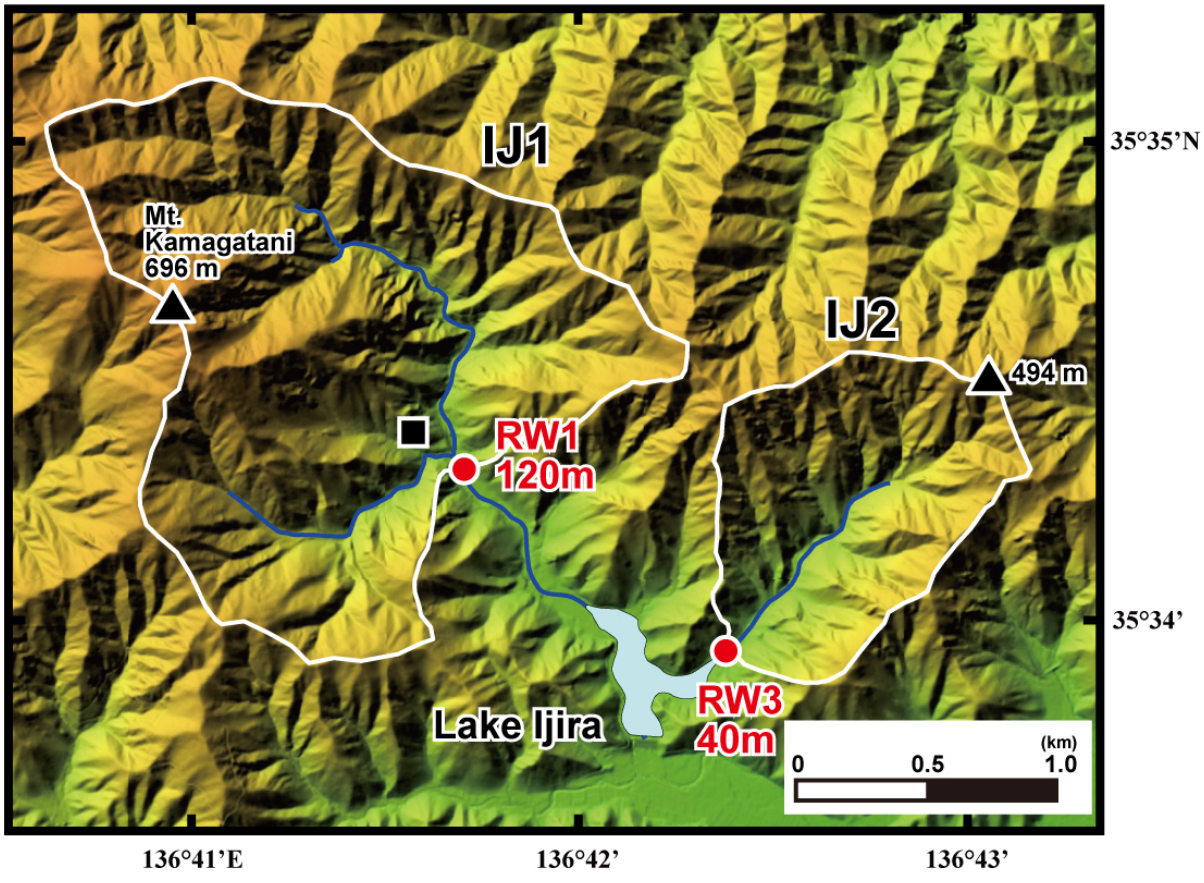

Figure 2: A color altitude map of the Lake Ijira watershed, together with the catchment areas, shown by a white line of the studied sites (IJ1 and IJ2) and the stream water sampling points, shown by red circles (RW1 for IJ1 and RW3 for IJ2). The black square denotes the location where the deposition sampler was set.

Biogeosciences Discuss., https://doi.org/10.5194/bg-2018-258
Manuscript under review for journal Biogeosciences
Discussion started: 12 July 2018

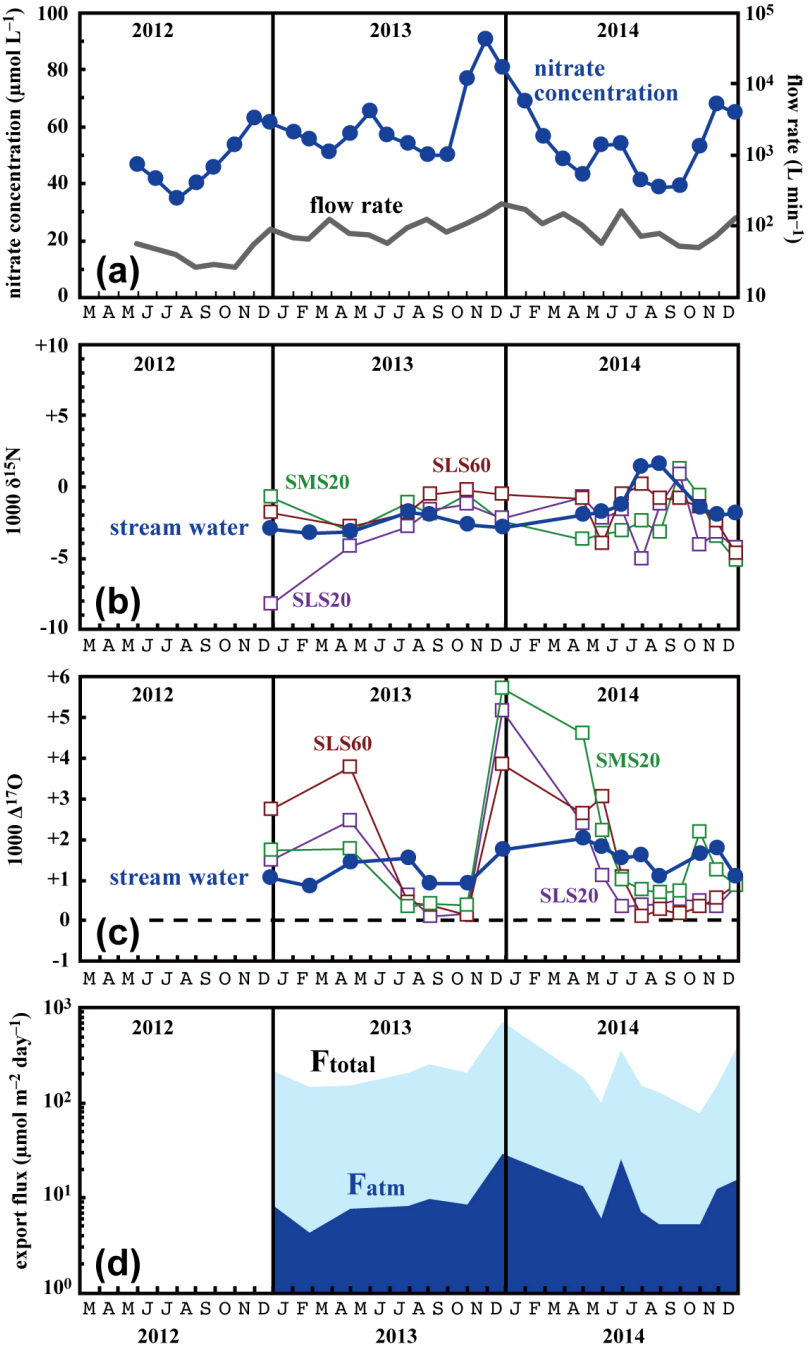

Figure 3: Temporal variations in the concentrations of nitrate (blue circles) and flow rates (grey line) in the stream water (a), together with those in the values of $\delta^{15}N$ (b), and $\Delta^{17}O$ (c) of the nitrate in stream and soil water, and in the export fluxes of nitrate (F_{total}) and atmospheric nitrate (F_{atm}) (d) via the stream at the KJ site.

Biogeosciences Discuss., https://doi.org/10.5194/bg-2018-258
Manuscript under review for journal Biogeosciences
Discussion started: 12 July 2018

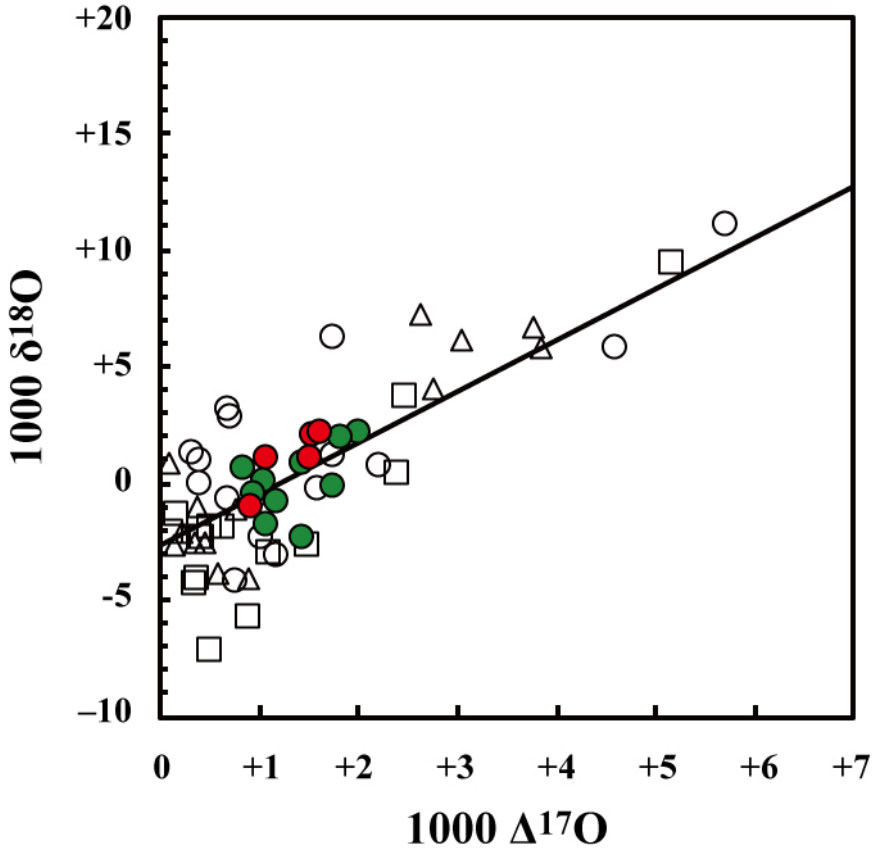

Figure 4: Relationship between $\Delta^{17}O$ and $\delta^{18}O$ values of nitrate in stream water at the KJ site (red circles: June, July, August, and September, green circles: rest of the months), together with those in soil water at the KJ site (SLS20: white squares, SLS60: white triangles, SMS20: white circles).

Biogeosciences Discuss., https://doi.org/10.5194/bg-2018-258
Manuscript under review for journal Biogeosciences
Discussion started: 12 July 2018

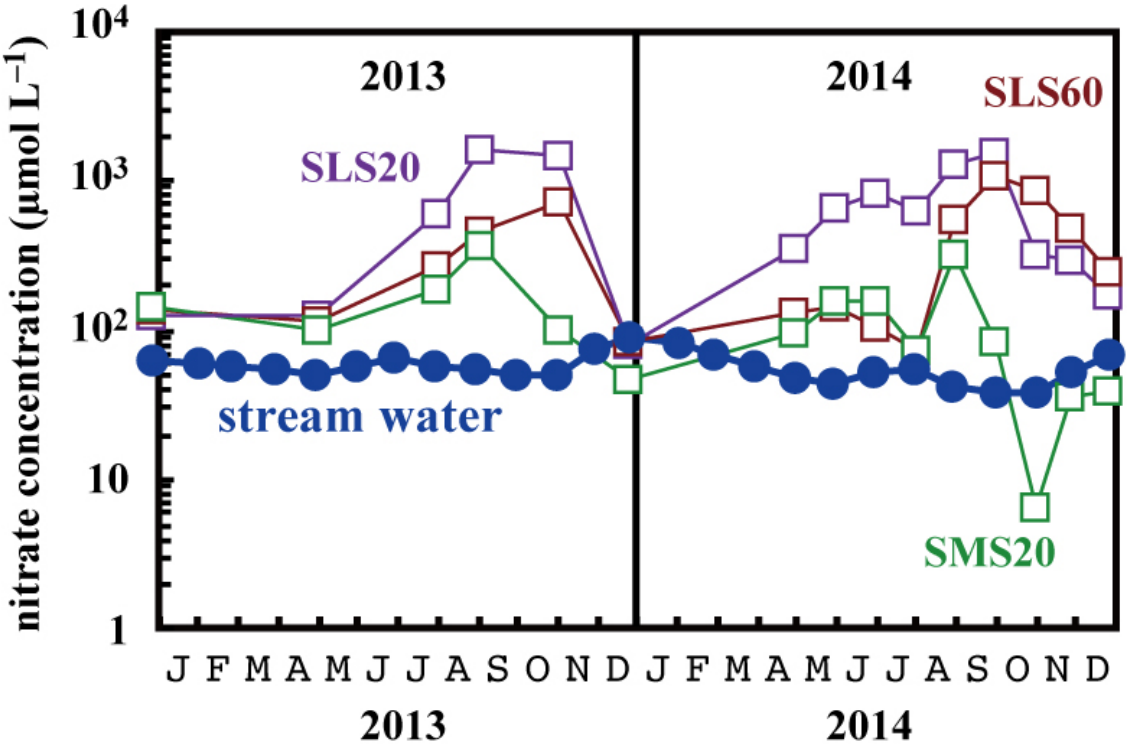

Figure 5: Temporal variations in the concentrations of nitrate in stream water (blue circles) and those in soil water (SMS20: green squares, SLS20: purple squares, SLS60: brown squares) at the KJ site on a logarithmic scale.

5

Biogeosciences Discuss., https://doi.org/10.5194/bg-2018-258
Manuscript under review for journal Biogeosciences
Discussion started: 12 July 2018

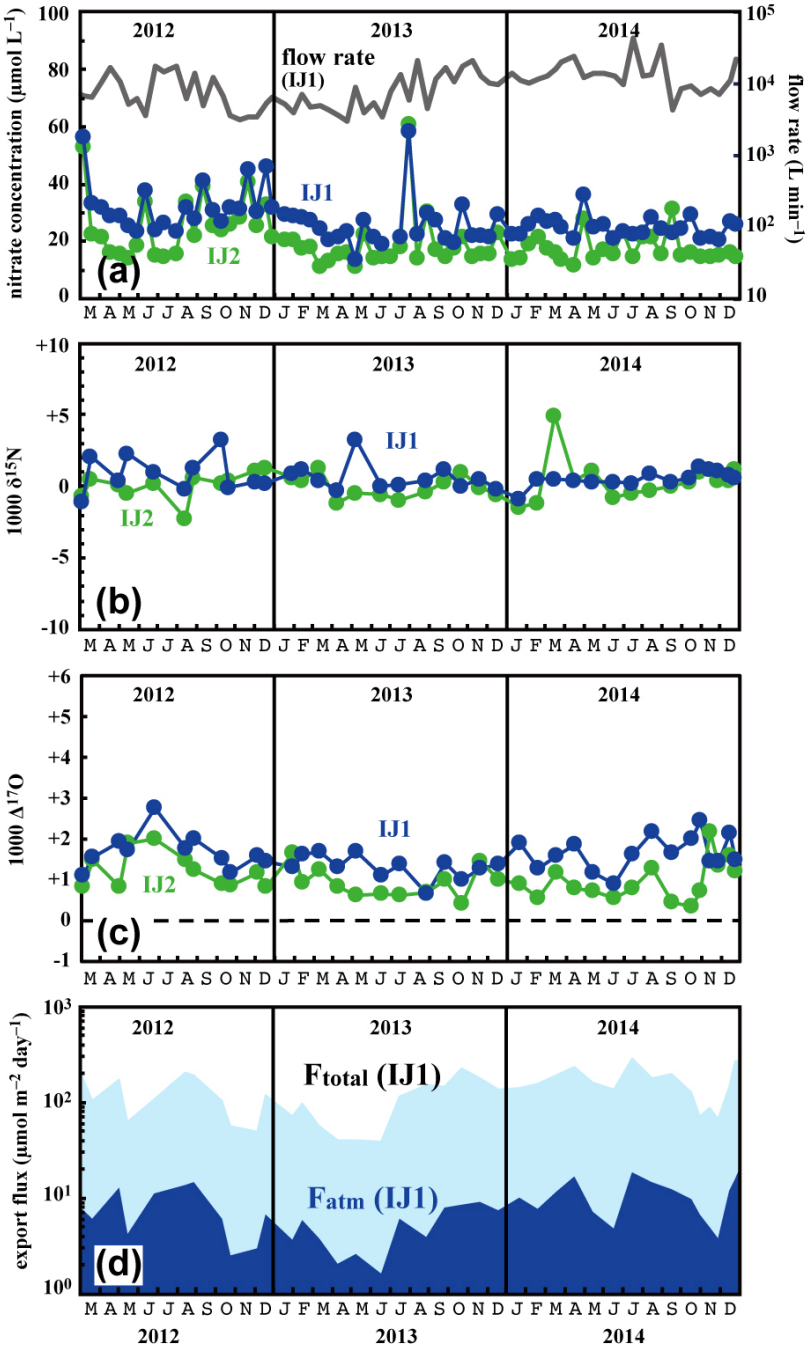

Figure 6: Temporal variations in concentrations of nitrate (IJ1: blue circles, IJ2: green circles) and flow rates at IJ1 (grey line) (a), together with those in the values of $\delta^{15}N$ (b), and $\Delta^{17}O$ (c) of nitrate at the IJ1 and IJ2 sites, and in the export fluxes of nitrate (F_{total}) and atmospheric nitrate (F_{atm}) via the stream at the IJ1 site (d).

Biogeosciences Discuss., https://doi.org/10.5194/bg-2018-258
Manuscript under review for journal Biogeosciences
Discussion started: 12 July 2018

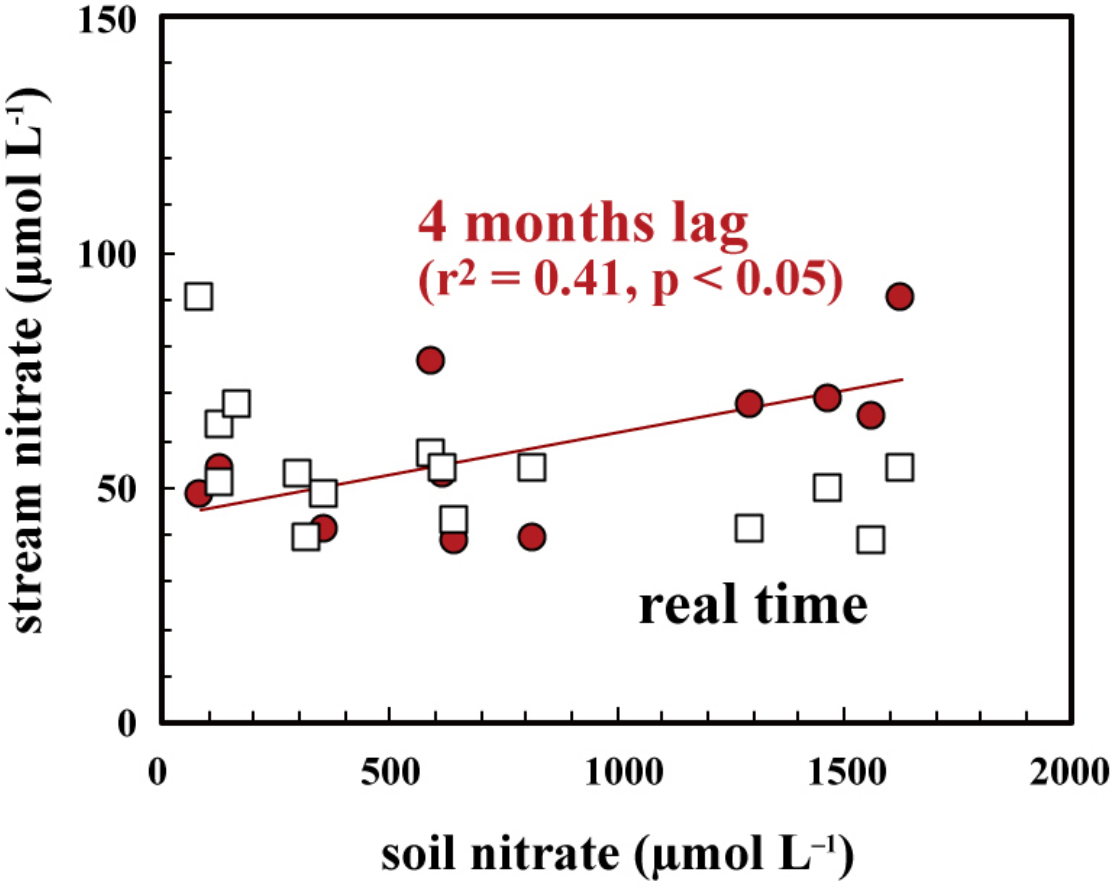

Figure 7: Relationship between concentrations of nitrate in soil water taken at SLS20 in KJ site and those in stream nitrate taken at the same time (white squares), together with those in stream nitrate taken 4 months later (red circles).

Biogeosciences Discuss., https://doi.org/10.5194/bg-2018-258
Manuscript under review for journal Biogeosciences
Discussion started: 12 July 2018

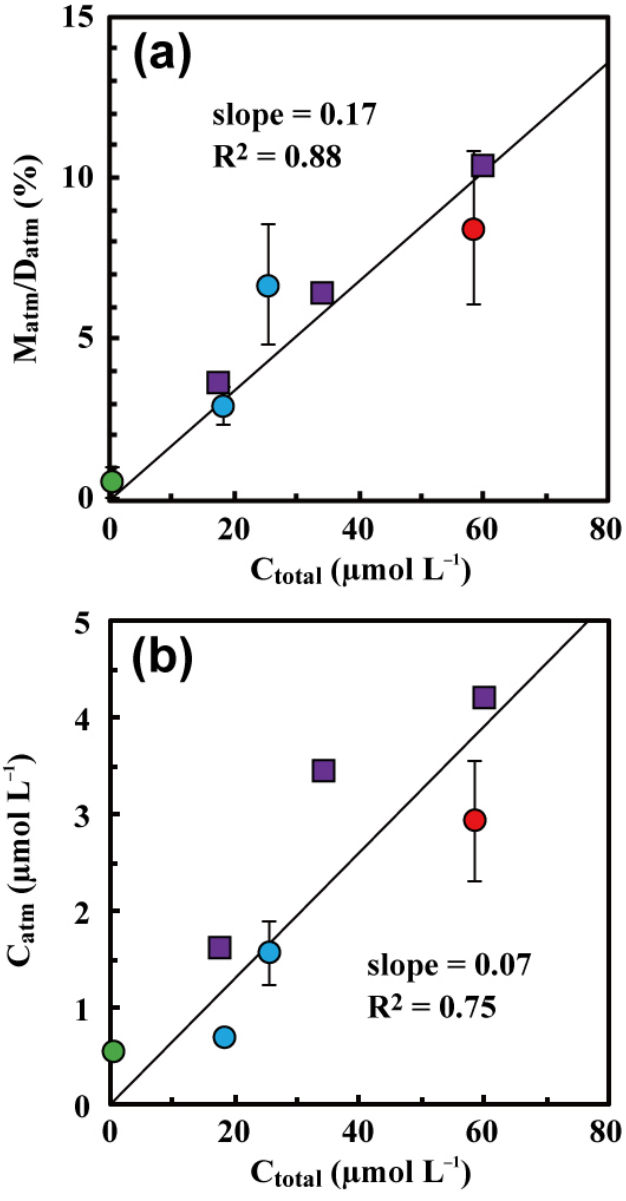

Figure 8: The annual export flux of unprocessed atmospheric nitrate relative to the annual deposition flux of atmospheric nitrate (M_{atm}/D_{atm} ratios) plotted as a function of the flux-weighted annual average concentration of nitrate in each stream water (C_{total}) (a); the flux-weighted annual average concentration of atmospheric nitrate in each stream water (C_{atm}) plotted as a function of the flux-weighted annual average concentration of nitrate in each stream water (C_{total}) (b) (KJ site: red circles, IJ1 and IJ2 sites: blue circles). Those determined at forested catchments in past studies are plotted as well, such as Fernow Experimental Forest in West Virginia, USA (purple squares; Rose et al., 2015a), and Teshio Experimental Forest in Hokkaido, Japan (a green circle; Tsunogai et al., 2014).

Biogeosciences Discuss., https://doi.org/10.5194/bg-2018-258
Manuscript under review for journal Biogeosciences
Discussion started: 12 July 2018

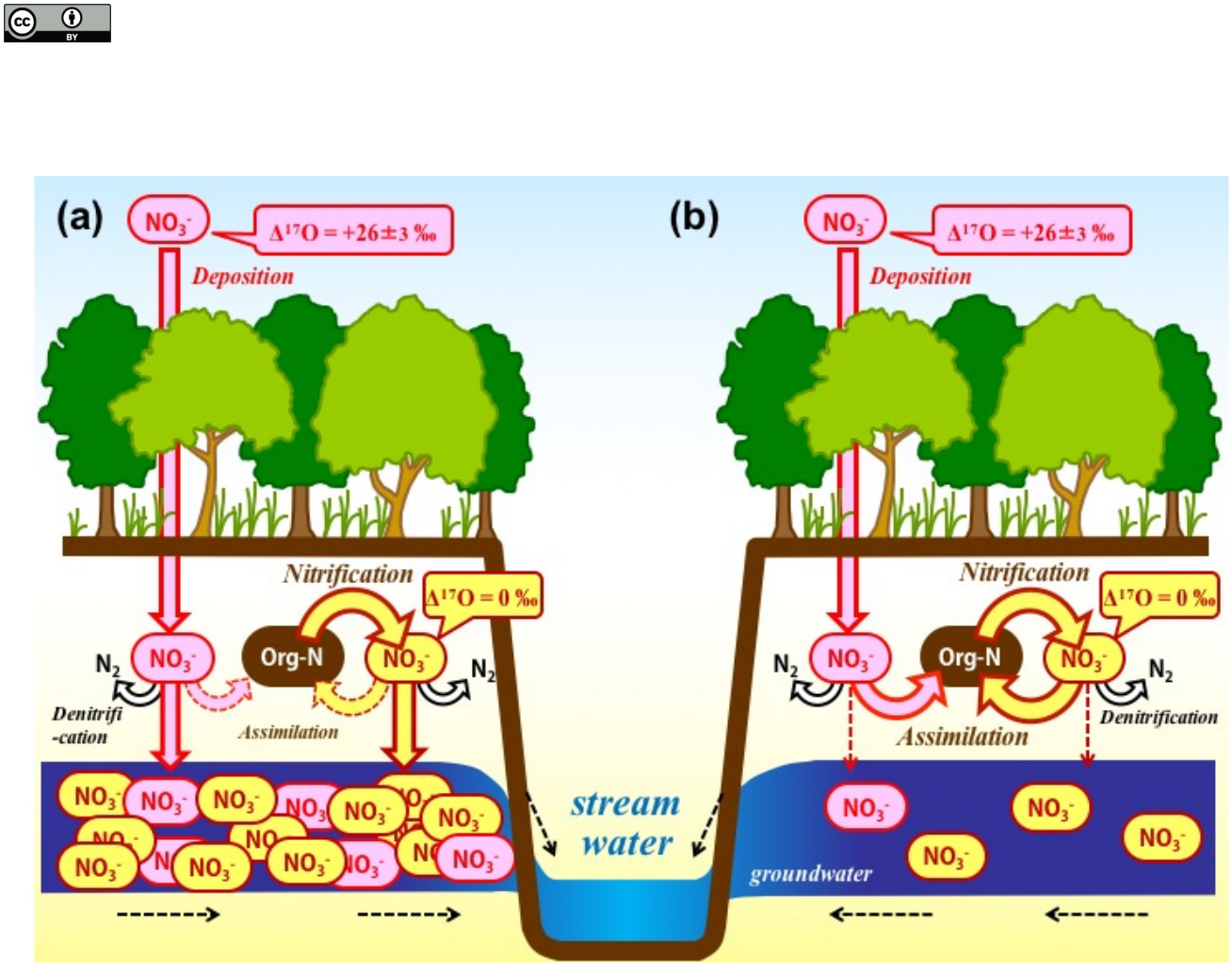

Figure 9: Schematic diagrams showing the biological processing of nitrate in a forested catchment under nitrogen saturation (a) and that under nitrogen limited, normal forest (b) (modified after Nakagawa et al., 2013).